JOURNAL OF BACTERIOLOGY, Dec. 2005, p. 8191–8195 Vol. 187, No. 23
0021-9193/05/$08.00+0 doi:10.1128/JB.187.23.8191–8195.2005

Four Unusual Two-Component Signal Transduction Homologs, RedC to RedF, Are Necessary for Timely Development in *Myxococcus xanthus*

Penelope I. Higgs,[1]† Kyungyun Cho,[2] David E. Whitworth,[3] Lisa S. Evans,[3] and David R. Zusman[1]*

Department of Molecular and Cell Biology, University of California, Berkeley, California 94720-3204[1]; Section of Life Science, Hoseo University, Asan 336-795, Korea[2]; and Department of Biological Sciences, University of Warwick, Gibbet Hill Road, Coventry CV4 7AL, United Kingdom[3]

Received 27 May 2005/Accepted 14 September 2005

We identified a cluster of four two-component signal transduction genes that are necessary for proper progression of *Myxococcus xanthus* through development. *redC* to *redF* mutants developed and sporulated early, resulting in small, numerous, and disorganized fruiting bodies. Yeast two-hybrid analyses suggest that RedCDEF act in a single signaling pathway. The previously identified *espA* gene displays a phenotype similar to that of *redCDEF*. However, combined mutants defective in *espA redCDEF* exhibited a striking additive developmental phenotype, suggesting that EspA and RedC to RedF play independent roles in controlling developmental progression.

Myxococcus xanthus is a gram-negative soil bacterium that exhibits a complex developmental program in which cells respond to starvation by first aggregating into mounds of approximately 100,000 cells and then, within these mounds, differentiating into spores (15). Previous work in our laboratory demonstrated that the timing of developmental progression in *M. xanthus* is modulated by EspA, a histidine kinase (HisKA) homolog (3). *espA* mutants develop earlier than wild-type cells, forming small, numerous fruiting bodies, with many spores outside of fruiting bodies. Epistasis analysis suggested that EspA functions downstream from EspB, a putative transport protein, in a signal transduction pathway. We hypothesized that EspA inhibits development until a signal is sensed that allows development to proceed. However, a cognate response regulator for EspA has not been identified, and the mechanism for regulation of developmental timing is unknown.

To identify additional genes in this regulatory pathway, we have employed a genetic screen to search for new mutations

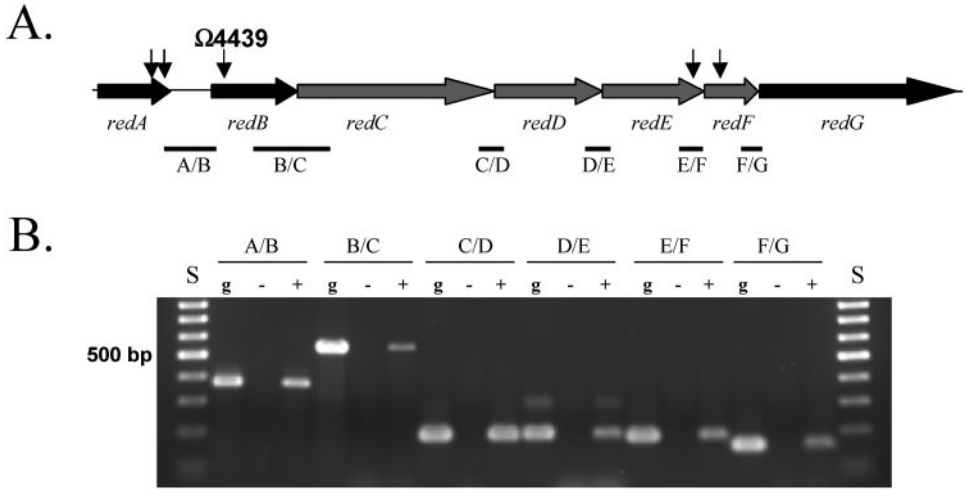

FIG. 1. Genetic arrangement of five independent transposons inserted into a single locus. A) Genetic arrangement of the *red* locus. Arrows indicate sites of *magellan4* transposon insertions. B) Analysis for polycistronic *red* mRNA by reverse transcriptase PCR. Intergenic regions between each gene (represented by bars in panel A) were amplified either from genomic DNA (g) or cDNA generated using RNA isolated from vegetatively growing cells in the presence (+) or absence (−) of reverse transcriptase. S, DNA size standards.

* Corresponding author. Mailing address: University of California, Department of Molecular and Cell Biology, 16 Barker Hall, Berkeley, CA 94720-3204. Phone: (501) 642-2293. Fax: (510) 643-6334. E-mail: zusman@uclink.berkeley.edu.

† Present address: Max Planck Institute for Terrestrial Microbiology, Karl-von-Frisch Str., 35043 Marburg, Germany.

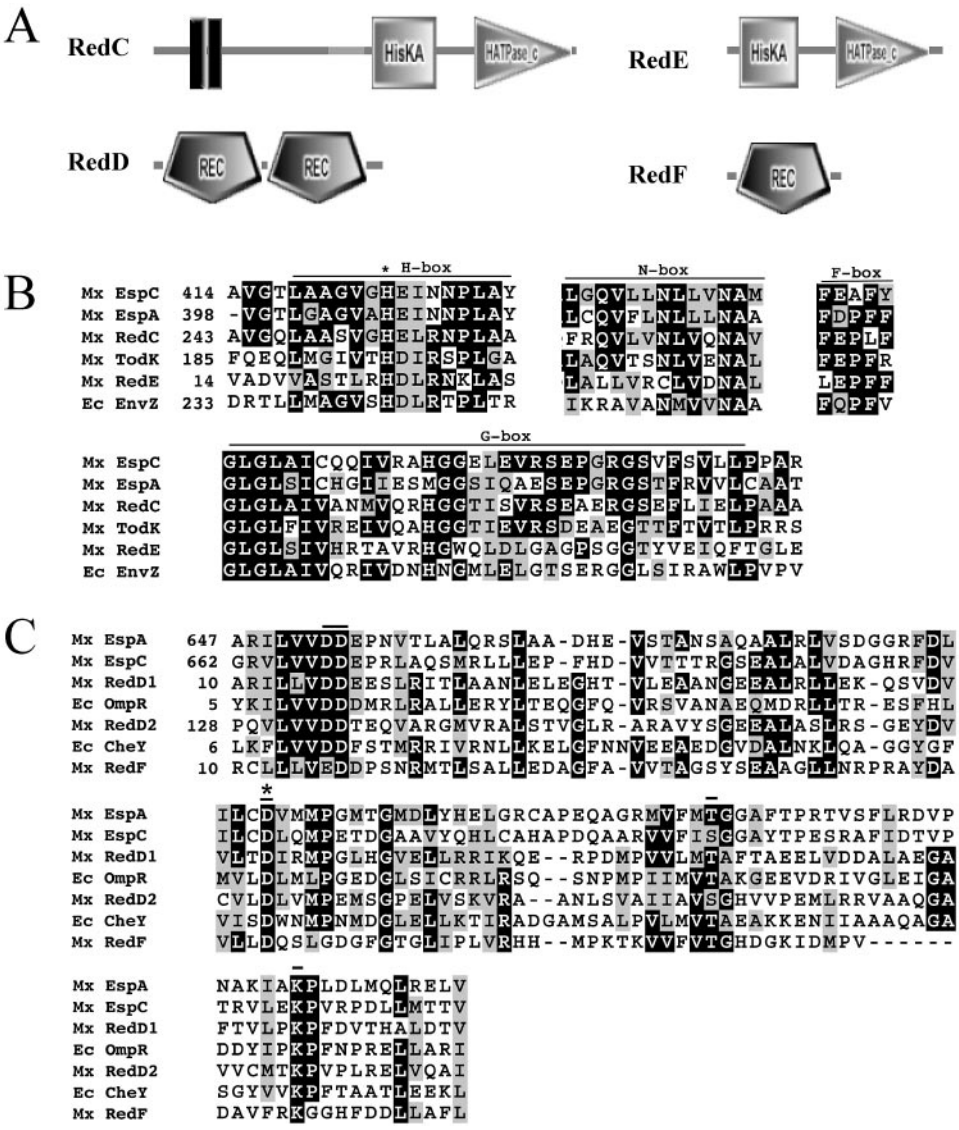

FIG. 2. Domain architecture and sequence alignments of histidine kinase and receiver domains. A) Arrangement of signal transduction domains of the two-component signal transduction proteins predicted by SMART. Histidine kinase (HisKA) and ATP-binding (HATPase_c) domains are depicted in RedC and RedE. Receiver (REC) domains are depicted in RedD and RedF. RedC was modified to add an additional transmembrane domain predicted by transmembrane hidden Markov model (16). B) Sequence alignments of RedC and RedD compared to several histidine kinases shown to modulate developmental progression in *M. xanthus* (EspC [9], EspA [3], TodK [12]) and to canonical histidine kinase EnvZ from *E. coli* (Ec EnvZ) (11). Conserved regions within the HisKA (H box) and HATPase_c (N, D, F, and G boxes) domains are shown. An asterisk denotes the conserved histidine residue which is the site of autophosphorylation in EnvZ (8). C) Receiver domains identified in RedD and RedF were aligned with those from the hybrid kinases EspA and EspC and canonical response regulator proteins OmpR and CheY from *E. coli*. Important functional residues are indicated by bars. An asterisk denotes the conserved aspartate residue which is the site of autophosphorylation in OmpR and CheY (19). Mx, *M. xanthus*; Ec, *E. coli*.

that cause an EspA-like phenotype (9). The screen involves using the *magellan4 mariner* transposon (13) to isolate mutants that sporulate early. We identified nine independent insertion mutants that showed this phenotype. One transposon insertion was mapped to the *espA* gene itself and a second insertion was mapped to *espC*, a hybrid histidine kinase that also functions to control the timing of fruiting body formation (9).

Identification of the *red* locus. Five of the nine *magellan4* insertion mutants were mapped (13) to a single locus consisting of at least seven genes (Fig. 1A). The locus was sequenced (GenBank accession number AY772188). Reverse transcriptase PCR analysis performed (18) on RNA isolated from vegetative cells indicated that these genes are part of an operon, since they are all expressed from a single transcript (Fig. 1B). The seven open reading frames were designated *redA* to *redF* (regulation of early development). BLAST (1) and SMART (10, 14) analysis of each open reading frame suggested that RedA contains a ribosomal SAE30/sigma 54 modulation domain, RedB contains no defined functional domains, and RedG contains a metallopeptidase domain. Interestingly,

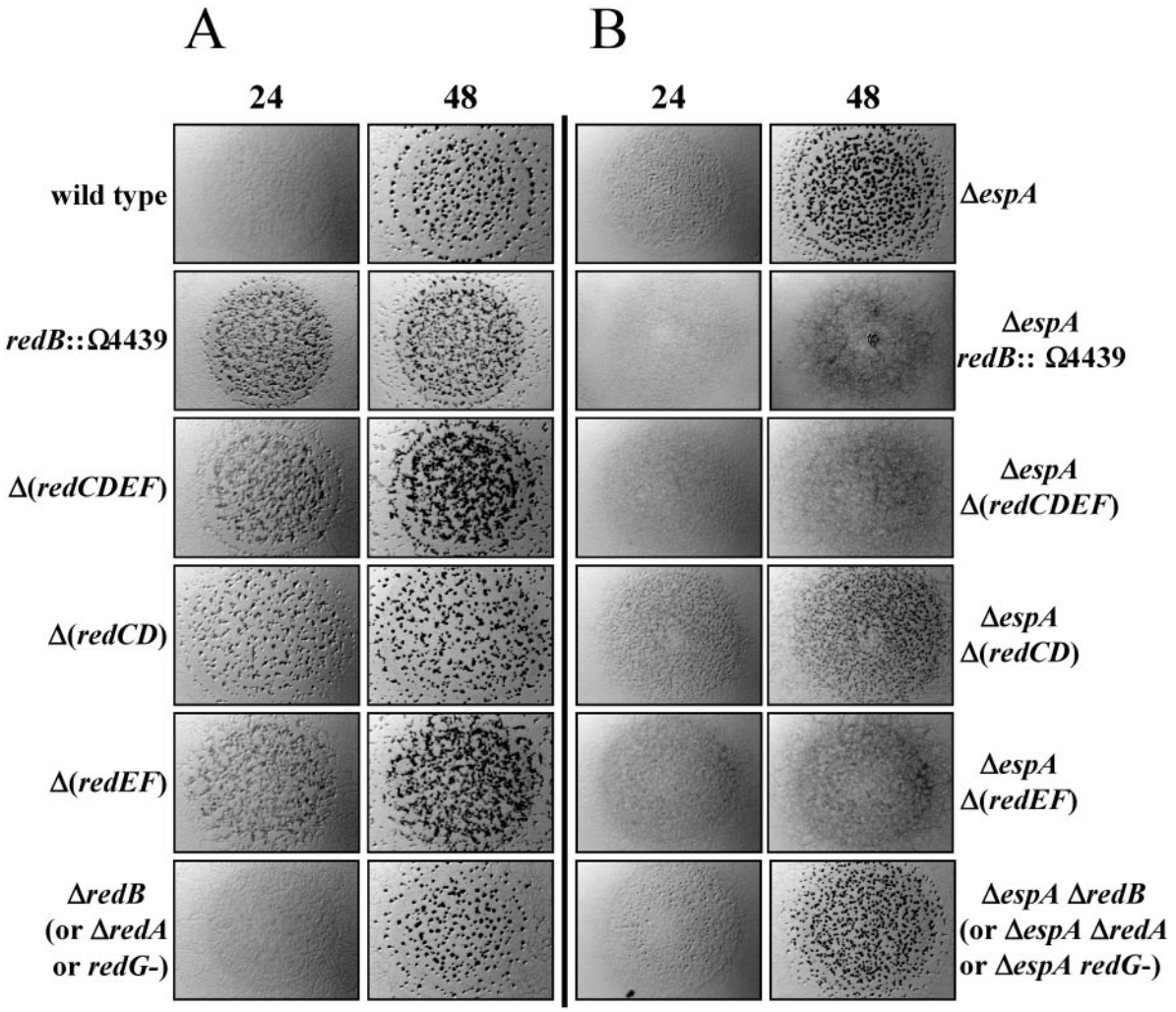

FIG. 3. Developmental phenotypes of *red* mutants. A) Developmental phenotypes of *redB*::Ω4439, Δ*redB*, Δ(*redCDEF*), Δ(*redCD*), and Δ(*redEF*) were analyzed in wild-type (DZ2) (DZ4657, DZ4663, DZ4659, DZ4665, or DZ4667, respectively) (A) or Δ*espA* (DZ4227) (DZ4658, DZ4664, DZ4660, DZ4666, or DZ4668, respectively) (B) backgrounds. Ten microliters of 2×10^9/ml cells was spotted on clone fruiting agar (18) and incubated at 32°C. Pictures were recorded at 24 and 48 h of development. Strains bearing Δ*redA* or an insertion in *redG* in the wild-type (DZ4661 or DZ4669, respectively) or Δ*espA* (DZ4662 or DZ4670, respectively) background behaved essentially as the respective Δ*redB* mutants with respect to fruiting body formation.

RedC to RedF appear to be two-component signal transduction proteins with unusual domain organization (Fig. 2A). Both RedD and RedF lack predicted DNA-binding elements, suggesting that they are not directly involved in regulating transcription. Sequence alignments indicate that RedC to RedF contain the conserved functional residues necessary for kinase and receiver function (5, 19), although the carboxy-terminal end of the RedF receiver domain contains either a truncation or deletion such that a conserved lysine residue is not positionally conserved (Fig. 2B and C).

Interruptions in the *red* locus accelerate both aggregation and sporulation during development. The *redB*::Ω4439 mutant (Fig. 1A) was backcrossed into the wild-type DZ2 strain (3), generating DZ4657, and the developmental phenotype was analyzed (Fig. 3A). DZ4657 cells aggregated earlier than the wild type and formed fruiting bodies that were small and numerous (Fig. 3A). Sporulation in the mutant was also early and yielded approximately 25% more spores than the wild type (Fig. 4A). These observations suggest that the *red* locus serves to inhibit progression of the developmental program until an unidentified condition, or set of conditions, is met.

***red* and *espA* mutant phenotypes are additive with respect to developmental timing.** To determine whether *espA* and *red* function in the same signaling pathway, we analyzed the phenotype of a Δ*espA redB*::Ω4439 double mutant (DZ4658) generated by introducing *redB*::Ω4439 into DZ4227 (3), a Δ*espA* strain. Surprisingly, although both mutations by themselves cause accelerated and more numerous fruiting bodies, the double mutant failed to form visible fruiting bodies under the conditions tested here (Fig. 3B); however, heat- and sonication-resistant spores were formed more than 48 h earlier than with the wild type and at least 24 h earlier than with either Δ*espA* or *redB*::Ω4439 single mutant (Fig. 4A). The *espA redB*::Ω4439 double mutant ultimately formed 1.5 times as many

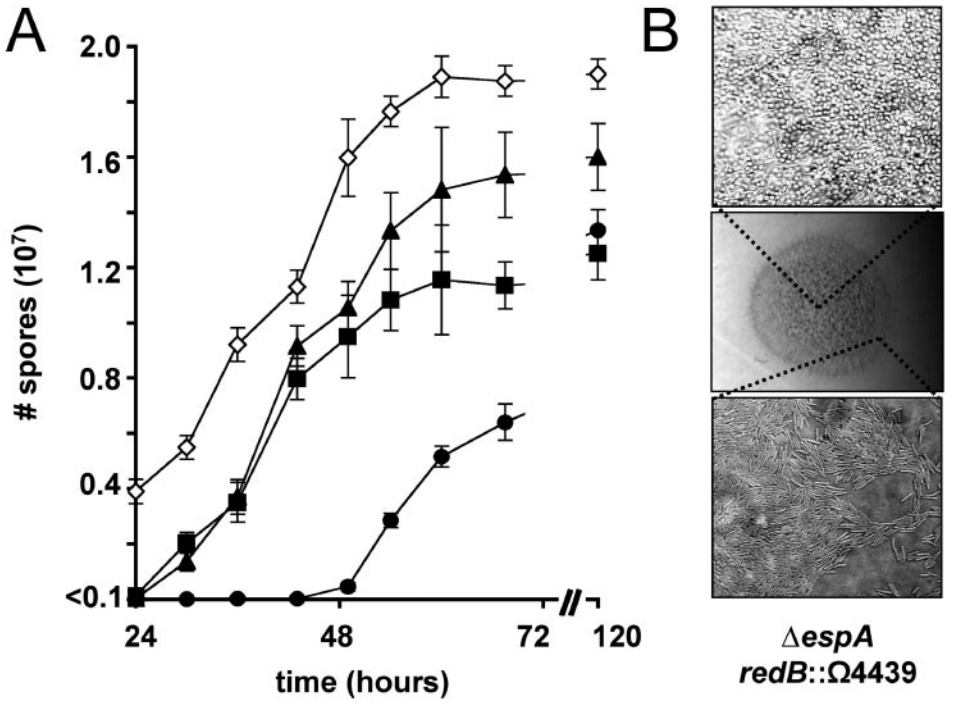

FIG. 4. Timing of spore formation during development in *redB*::Ω4439. A) Spore production during the first 70 h of development. Ten microliters of 2×10^9 cells/ml of wild-type (solid circles), *redB*::Ω4439 (solid triangles), Δ*espA* (solid squares), or Δ*espA redB*::Ω4439 (open diamonds) cells were spotted in triplicate on clone fruiting media and incubated at 32°C. Cells were harvested at the indicated time points, and the number of heat- and sonication-resistant spores (3) was determined. B) Δ*espA redB*::Ω4439 (DZ4658) cells after 72 h of development pictured at 12× magnification (center panel) and 1,000× magnification of the swarm edge (bottom panel), demonstrating undifferentiated cells and the center of the spot (top panel) showing lawns of spores.

spores as the wild type or the *espA* single mutant and 1.25 times as many spores as the *redB*::Ω4439 mutants. The additive defects observed in the double mutants of timing and total spore production suggest that *espA* and the *red* loci independently inhibit development progression.

Examination of the spots of developing Δ*espA redB*::Ω4439 mutants under higher magnification revealed that these cells differentiated into thin layers of spores (Fig. 4B), but as observed with wild-type cells, they remained as rods near the edge of the spot, presumably because cells at this location are not sensing the same degree of starvation as cells at the center of the spot or, alternatively, because the population density is lower there. The Δ*espA redB*::Ω4439 double mutants exhibited growth rates identical to those of the wild type under high- or low-nutrient conditions (Casitone-yeast extract [CYE] [18], CYE lacking yeast extract, or the latter medium with Casitone reduced to 0.5% or 0.25%). The double mutants also showed no signs of development when incubated under vegetative conditions, shaking in liquid starvation media, or at low cell density on starvation media (data not shown). These observations suggest that these cells were still responding appropriately to signals required for the initiation of development and that the double mutant phenotype arises from the combined loss of two inhibitors of developmental progression rather than a defect in nutrient sensing.

The *redCDEF* genes are necessary for timely development. Since the *red* genes are part of an operon, the *redB*::Ω4439 mutant is likely to be polar on the expression of downstream genes. To analyze these genes further, we constructed in-frame deletions (7) in *redC* to *redF*, *redA*, or *redB* (DZ4659, DZ4661, and DZ4663, respectively) and an insertion in *redG* (DZ4669). Phenotypic analysis of these mutants determined that only the Δ(*redCDEF*) deletion displayed the *redB*::Ω4439 mutant phenotype (Fig. 3A and data not shown). Additionally, when these deletions were introduced into a Δ*espA* strain, only the Δ*espA* Δ(*redCDEF*) mutant (DZ4660) showed the early-sporulation, nonaggregation phenotype (Fig. 3B and data not shown). These results suggest that RedC to RedF two-component signal transduction proteins regulate the timing of development, while RedA, RedB, and RedG have unknown functions.

***redEF* mutants are epistatic to *redCD* mutants.** We next constructed and analyzed Δ(*redCD*) (DZ4665) and Δ(*redEF*) (DZ4667) mutants. Both the Δ(*redCD*) and Δ(*redEF*) mutants aggregated early, but the resulting fruiting bodies were less numerous and more organized in the Δ(*redCD*) mutant than in the Δ(*redEF*) mutant (Fig. 3A). In addition, only Δ*espA* Δ(*redEF*) (DZ4668) double mutants formed the early-sporulation, nonaggregation phenotype; Δ*espA* Δ(*redCD*) (DZ4666) double mutants still formed fruiting bodies, albeit even smaller and more numerous than either single mutant alone (Fig. 3B). In both the wild-type and Δ*espA* backgrounds, the Δ(*redEF*) mutants phenocopy the Δ(*redCDEF*) mutants with respect to fruiting body appearance (Fig. 3) and timing of sporulation (data not shown), indicating that *redEF* is epistatic over *redCD*. These results suggest that RedEF may act downstream of RedCD in a signal transduction pathway.

RedD interacts with both RedC and RedE in a yeast two-hybrid interaction assay. When all possible combinations of Red histidine kinase (HisKA) and receiver (REC) domains were analyzed for interactions in the yeast two-hybrid system

TABLE 1. Yeast two-hybrid interaction analysis[a]

Bait protein	Domain	Prey protein and domain							
		RedC, HisKA	RedD, REC1	RedD, REC2	RedE, HisKA	RedF, REC	FrzZ, REC1	FrzZ, REC2	RNM
RedC	HisKA	++	±	+	−	±	−	−	−
RedD	REC1	−	−	−	++	−	−	−	−
RedD	REC2	−	±	±	±	−	−	−	−
RedE	HisKA	−	+	−	−	−	−	−	−
RedF	REC	−	−	−	++	−	−	−	−
FrzZ	REC1	−	−	−	−	−	−	−	−
FrzZ	REC2	−	−	−	−	−	−	−	−
QN		−	−	−	−	−	−	−	++

[a] Plasmids encoding B42 activation domain (prey, pJG4-5) (6) fusions to the histidine kinase (HisKA) domains of RedC (pLSE16) and RedE (pLSE19) and the receiver (REC) domains of RedD (REC1, pLSE17; REC2, pLSE18) and RedF (pLSE20) were paired with plasmids encoding the respective LexA binding domain (bait, pEG202) (6) fusions (pLSE06, pLSE07, pLSE08, pLSE09, or pLSE10) in the *Saccharomyces cerevisiae* EGY48/pSH18-34 *lacZ* reporter strain (4, 6) and tested for relative beta-galactosidase activity in the presence of galactose and 5-bromo-4-chloro-3-indolyl-β-D-galactopyranoside after 72 h of growth. Strong positive interactions (++) were defined by RNW (pDEW020) and QN (pDEW002) (2). +, positive interaction; ±, insignificant interaction; −, no interaction.

(20), specific positive interactions were detected between the RedC HisKA domain and the second receiver domain of RedD (REC2) as bait and prey, respectively (Table 1). Likewise, a specific strongly positive interaction was also detected between the RedE HisKA domain and the RedF REC domain as prey and bait, respectively. In addition, strong positive and reciprocal interactions between the RedE HisKA domain and RedD REC1 were detected. These interactions were specific, since neither HisKA domain interacted positively with either receiver of FrzZ, another protein consisting of dual-receiver domains (17). These results are consistent with the genetic epistasis experiments and suggest that RedC to RedF participate in an unusual signal transduction pathway which, distinct from the EspA signaling pathway, controls developmental timing in *M. xanthus*. We are currently investigating the molecular mechanisms by which this control is mediated.

Nucleotide sequence accession number. The sequence of the *red* locus was deposited in GenBank under accession no. AY772188.

The authors gratefully acknowledge Andrew Millard for assistance with yeast two-hybrid assays and past and present members of the Zusman laboratory for helpful discussions and critical reading of the manuscript.

This work was supported by grants from the National Institutes of Health (GM64463 and GM20509) to D.Z.

REFERENCES

1. **Altschul, S. F., T. L. Madden, A. A. Schaffer, J. Zhang, Z. Zhang, W. Miller, and D. J. Lipman.** 1997. Gapped BLAST and PSI-BLAST: a new generation of protein database search programs. Nucleic Acids Res. **25:**3389–3402.
2. **Browning, D. F., D. E. Whitworth, and D. A. Hodgson.** 2003. Light-induced carotenogenesis in Myxococcus xanthus: functional characterization of the ECF sigma factor CarQ and antisigma factor CarR. Mol. Microbiol. **48:**237–251.
3. **Cho, K., and D. R. Zusman.** 1999. Sporulation timing in *Myxococcus xanthus* is controlled by the *espAB* locus. Mol. Microbiol. **34:**714–725.
4. **Estojak, J., R. Brent, and E. A. Golemis.** 1995. Correlation of two-hybrid affinity data with in vitro measurements. Mol. Cell. Biol. **15:**5820–5829.
5. **Grebe, T. W., and J. B. Stock.** 1999. The histidine protein kinase superfamily. Adv. Microb. Physiol. **41:**139–227.
6. **Gyuris, J., E. Golemis, H. Chertkov, and R. Brent.** 1993. Cdi1, a human G1 and S phase protein phosphatase that associates with Cdk2. Cell **75:**791–803.
7. **Julien, B., A. D. Kaiser, and A. Garza.** 2000. Spatial control of cell differentiation in Myxococcus xanthus. Proc. Natl. Acad. Sci. USA **97:**9098–9103.
8. **Kanamaru, K., H. Aiba, and T. Mizuno.** 1990. Transmembrane signal transduction and osmoregulation in Escherichia coli: I. Analysis by site-directed mutagenesis of the amino acid residues involved in phosphotransfer between the two regulatory components, EnvZ and OmpR. J. Biochem. (Tokyo) **108:**483–487.
9. **Lee, B., P. I. Higgs, D. R. Zusman, and K. Cho.** 2005. EspC is involved in controlling the timing of development in *Myxococcus xanthus*. J. Bacteriol. **187:**5029–5031.
10. **Letunic, I., R. R. Copley, S. Schmidt, F. D. Ciccarelli, T. Doerks, J. Schultz, C. P. Ponting, and P. Bork.** 2004. SMART 4.0: towards genomic data integration. Nucleic Acids Res. **32:**D142–D144.
11. **Mizuno, T., E. T. Wurtzel, and M. Inouye.** 1982. Osmoregulation of gene expression. II. DNA sequence of the envZ gene of the ompB operon of Escherichia coli and characterization of its gene product. J. Biol. Chem. **257:**13692–13698.
12. **Rasmussen, A. A., and L. Sogaard-Andersen.** 2003. TodK, a putative histidine protein kinase, regulates timing of fruiting body morphogenesis in *Myxococcus xanthus*. J. Bacteriol. **185:**5452–5464.
13. **Rubin, E. J., B. J. Akerley, V. N. Novik, D. J. Lampe, R. N. Husson, and J. J. Mekalanos.** 1999. In vivo transposition of mariner-based elements in enteric bacteria and mycobacteria. Proc. Natl. Acad. Sci. USA **96:**1645–1650.
14. **Schultz, J., F. Milpetz, P. Bork, and C. P. Ponting.** 1998. SMART, a simple modular architecture research tool: identification of signaling domains. Proc. Natl. Acad. Sci. USA **95:**5857–5864.
15. **Shimkets, L. J.** 1990. Social and developmental biology of the myxobacteria. Microbiol. Rev. **54:**473–501.
16. **Sonnhammer, E. L., G. von Heijne, and A. Krogh.** 1998. A hidden Markov model for predicting transmembrane helices in protein sequences. Proc. Int. Conf. Intell. Syst. Mol. Biol. **6:**175–182.
17. **Trudeau, K. G., M. J. Ward, and D. R. Zusman.** 1996. Identification and characterization of FrzZ, a novel response regulator necessary for swarming and fruiting-body formation in Myxococcus xanthus. Mol. Microbiol. **20:**645–655.
18. **Vlamakis, H. C., J. R. Kirby, and D. R. Zusman.** 2004. The Che4 pathway of Myxococcus xanthus regulates type IV pilus-mediated motility. Mol. Microbiol. **52:**1799–1811.
19. **Volz, K.** 1993. Structural conservation in the CheY superfamily. Biochemistry **32:**11741–11753.
20. **Whitworth, D. E., and D. A. Hodgson.** 2001. Light-induced carotenogenesis in Myxococcus xanthus: evidence that CarS acts as an anti-repressor of CarA. Mol. Microbiol. **42:**809–819.